



HAL
open science

Rotational spectroscopy of isotopic cyclopropenone, c-H₂C₃O, and determination of its equilibrium structure

Holger S. P. Mueller, Ananya M. Brahmi, Jean-Claude Guillemin, Frank Lewen, Stephan Schlemmer

► **To cite this version:**

Holger S. P. Mueller, Ananya M. Brahmi, Jean-Claude Guillemin, Frank Lewen, Stephan Schlemmer. Rotational spectroscopy of isotopic cyclopropenone, c-H₂C₃O, and determination of its equilibrium structure. *Astronomy and Astrophysics - A&A*, 2021, 647, pp.A179. 10.1051/0004-6361/202040088 . hal-03217061

HAL Id: hal-03217061

<https://hal.science/hal-03217061v1>

Submitted on 17 Nov 2021

HAL is a multi-disciplinary open access archive for the deposit and dissemination of scientific research documents, whether they are published or not. The documents may come from teaching and research institutions in France or abroad, or from public or private research centers.

L'archive ouverte pluridisciplinaire **HAL**, est destinée au dépôt et à la diffusion de documents scientifiques de niveau recherche, publiés ou non, émanant des établissements d'enseignement et de recherche français ou étrangers, des laboratoires publics ou privés.

Rotational spectroscopy of isotopic cyclopropanone, $c\text{-H}_2\text{C}_3\text{O}$, and determination of its equilibrium structure[★]

Holger S. P. Müller¹, Ananya Brahma M.¹, Jean-Claude Guillemin², Frank Lewen¹, and Stephan Schlemmer¹

¹ I. Physikalisches Institut, Universität zu Köln, Zùlpicher Str. 77, 50937 Köln, Germany
e-mail: hspm@ph1.uni-koeln.de

² Univ Rennes, Ecole Nationale Supérieure de Chimie de Rennes, CNRS, ISCR-UMR 6226, 35000 Rennes, France

Received XX YYY 2021 / Accepted XX YYY 2021

ABSTRACT

Context. Cyclopropanone was first detected in the cold and less dense envelope of the giant molecular cloud Sagittarius B2(N). It was found later in several cold dark clouds. It may be possible to detect its minor isotopic species in these environments. In addition, the main species may well be identified in warmer environments.

Aims. We want to extend existing line lists of isotopologs of $c\text{-H}_2\text{C}_3\text{O}$ from the microwave to the millimeter region and create one for the singly deuterated isotopolog to facilitate their detections in space. Furthermore, we want to extend the line list of the main isotopic species to the submillimeter region and to evaluate an equilibrium structure of the molecule.

Methods. We employed a cyclopropanone sample in natural isotopic composition to investigate the rotational spectra of the main and ¹⁸O-containing isotopologs as well as the two isotopomers containing one ¹³C atom. Spectral recordings of the singly and doubly deuterated isotopic species were obtained using a cyclopropanone sample highly enriched in deuterium. We recorded rotational transitions in the 70–126 GHz and 160–245 GHz region for all isotopologs and for the main species also in the 342–505 GHz range. Quantum-chemical calculations were carried out to evaluate initial spectroscopic parameters and the differences between ground state and equilibrium rotational parameters to derive semi-empirical equilibrium structural parameters.

Results. We determined new or improved spectroscopic parameters for six isotopologs and structural parameters according to different structure models.

Conclusions. The spectroscopic parameters are accurate enough to identify minor isotopic species at centimeter and millimeter wavelengths while those of the main species are deemed to be reliable up to 1 THz. Our structural parameters differ from earlier ones. The deviations are attributed to misassignments in the earlier spectrum of one isotopic species.

Key words. Molecular data – Methods: laboratory: molecular – Techniques: spectroscopic – Radio lines: ISM – ISM: molecules – Astrochemistry

1. Introduction

Cyclopropanone is one of the smallest aromatic molecules (Anonymous 1983; Wang et al. 2011), after cyclopropenylidene ($c\text{-C}_3\text{H}_2$), and the first cyclic molecule with a ketone functional group which was detected in space. It was first found in the cold and less dense envelope of the giant star-forming region Sagittarius B2(N) (Hollis et al. 2006). More recently, $c\text{-H}_2\text{C}_3\text{O}$ was detected in four dark clouds or prestellar cores, TMC-1, B1-b, L483, and Lupus-1A (Loison et al. 2016). It was found in addition in the low-mass star-forming region L1527 (Araki et al. 2017).

Benson et al. (1973) presented the first account on the rotational spectrum of cyclopropanone. They reported between 6 and 14 rotational transitions for five isotopic species recorded between 9 GHz and 40 GHz. The main isotopolog and the two isotopomers containing one ¹³C atom were studied in a sample in natural isotopic composition. They employed isotopic en-

riched samples for the investigations of the isotopologs containing ¹⁸O or two D. Additionally, they derived structural parameters of $c\text{-H}_2\text{C}_3\text{O}$ and determined its dipole moment and rotational g values through Stark and Zeeman measurements, respectively. Later, Guillemin et al. (1990) extended the data set of the main isotopic species to 247 GHz. These data are sufficient to identify $c\text{-H}_2\text{C}_3\text{O}$ in cold astronomical sources up to the lower submillimeter region, possibly up to ~500 GHz, but are not enough for searches in warmer astronomical environments. Although cyclopropanone was identified to date only in colder sources, it may well be detected in the warmer and denser parts of star-forming regions one day. Propanal (Lykke et al. 2017), propene, and propenal (Manigand et al. 2021) are recent examples of molecules initially found only in cold astronomical sources later found in the hot corino, the warmer and denser parts of a low-mass star-forming region, of IRAS 16293–2422 B in these cases. The isotopic data may be suitable for astronomical searches in cold environments in the microwave and possibly lower millimeter regions if good estimates of the lowest order centrifugal distortion parameters are available, but are certainly too limited for searches throughout the entire millimeter region. Moreover, no data are available for $c\text{-HDC}_3\text{O}$, which is the most promising isotopolog to be found in cold dark molecular clouds. Therefore, we investigated the rotational spectra of

[★] Transition frequencies from this work as well as related data from earlier work are given for each isotopic species as supplementary material. Given are also quantum numbers, uncertainties, and residuals between measured frequencies and those calculated from the final sets of spectroscopic parameters. The data are available at CDS via anonymous ftp to cdsarc.u-strasbg.fr (130.79.128.5) or via <http://cdsweb.u-strasbg.fr/cgi-bin/qcat?J/A+A/>

five isotopologs of cyclopropanone in the millimeter region to facilitate their detection in space and extended measurements of the main isotopic species to the lower submillimeter region to allow more secure searches in warmer astronomical sources.

2. Experimental details

2.1. Sample preparation

The synthesis of normal cyclopropanone was the same as in Guillemin et al. (1990) and followed the procedure described by Breslow et al. (1977). The synthesis of the cyclopropanone sample highly enriched in deuterium followed largely Breslow & Oda (1972) with $n\text{-Bu}_3\text{SnH}$ replaced by $n\text{-Bu}_3\text{SnD}$. Please note that cyclopropanone decomposes at room temperature. It is very stable in a sealed container at temperatures below ~ 240 K. We kept the sample at dry ice or liquid nitrogen temperature in our experiments.

2.2. Spectroscopic measurements

The investigation of the rotational spectra of cyclopropanone isotopologs was carried out with two different spectrometers. We employed two 7 m long coupled glass cells with 10 cm inner diameter in a double path arrangement for measurements in the 70–126 GHz region, yielding an optical path length of 28 m. We used a 5 m long double path cell with 10 cm inner diameter for the 160–245 GHz and the 342–505 GHz ranges. Both spectrometers use Virginia Diode, Inc. (VDI), frequency multipliers driven by Rohde & Schwarz SMF 100A synthesizers as sources and Schottky diode detectors. Frequency modulation was employed to reduce baseline effects with demodulation at twice the modulation frequency. This causes absorption lines to appear approximately as second derivatives of a Gaussian. Additional information on the spectrometers are available in Ordu et al. (2012) and Martin-Drumel et al. (2015), respectively.

We recorded individual transition frequencies in all three frequency windows covering 10 MHz for well-predicted lines up to 100 MHz in the search for first lines of the singly deuterated isotopolog. The pressure was around 1.0 Pa in the 3 mm region as test measurements showed that the peak intensity was best between ~ 0.75 and ~ 1.5 Pa. The pressure was between 1.0 and 2.0 Pa at shorter wavelengths. We refilled the cells after roughly one hour because the molecule is only moderately stable at room temperature; its half-life was close to one hour in our cells. Uncertainties were evaluated mostly based on the symmetry of the line shape and were as small as 5 kHz for isolated and very symmetric lines. Such small uncertainties were achieved earlier, for example, in the case of 2-cyanobutane with a much richer rotational spectrum (Müller et al. 2017). **Uncertainties for good lines were 10–20 kHz, and larger ones, up to ~ 100 kHz, were used for example for weaker lines and lines close to other lines.**

Initial measurements using the highly deuterated cyclopropanone sample yielded no clear signs of rotational transitions of $c\text{-D}_2\text{C}_3\text{O}$, but instead strong signals of $c\text{-H}_2\text{C}_3\text{O}$. We suspected rapid D-to-H exchange on the cell walls, even though this may appear unusual for a molecule with substantial aromatic character. On the other hand, at least some unsaturated molecules are known to exchange D and H quite readily; for example, the reaction between HC_3N and D_2O was used to generate DC_3N (Spahn et al. 2008). We conditioned the cell walls with ~ 200 Pa D_2O for two hours and observed strong signals of $c\text{-D}_2\text{C}_3\text{O}$ and very weak ones of $c\text{-H}_2\text{C}_3\text{O}$ afterwards. The sig-

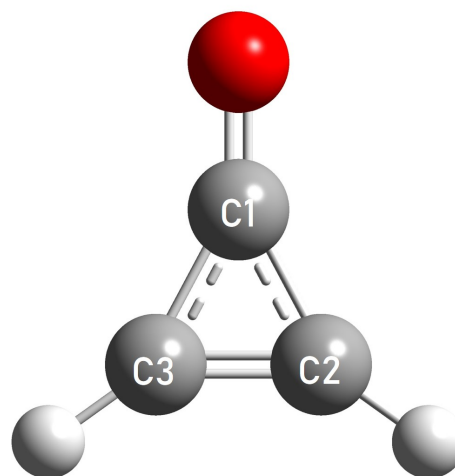


Fig. 1. Model of the cyclopropanone molecule. Carbon atoms are symbolized by gray spheres which are numbered. Hydrogen atoms are indicated by small, light gray spheres and the oxygen atom by a red sphere.

nals of $c\text{-HDC}_3\text{O}$, identified later, were in between, roughly a factor of four weaker than those of $c\text{-D}_2\text{C}_3\text{O}$.

3. Quantum-chemical calculations

We carried out quantum-chemical calculations at the Regionales Rechenzentrum der Universität zu Köln (RRZK) using the commercially available program Gaussian 09 (Frisch et al. 2013). We performed B3LYP hybrid density functional (Becke 1993; Lee et al. 1988), Møller-Plesset second (MP2) and third order perturbation theory (MP3) calculations (Møller & Plesset 1934), along with coupled cluster calculations with singles and doubles excitations augmented by a perturbative correction for triple excitations, CCSD(T) (Raghavachari et al. 1989). We employed correlation consistent basis sets which were augmented with diffuse basis functions aug-cc-pVXZ ($X = \text{T}, \text{Q}, 5$) (Dunning, Jr. 1989), which we abbreviate here as 3a, 4a, and 5a, respectively. These basis sets were further augmented with core-correlating basis functions in some cases, yielding the aug-cc-pwCVXZ basis sets (Peterson & Dunning, Jr. 2002), which we denote as 3aC, 4aC, and 5aC, respectively.

Equilibrium geometries were determined by analytic gradient techniques, harmonic force fields by analytic second derivatives, and anharmonic force fields by numerical differentiation of the analytically evaluated second derivatives of the energy. The main goals of these anharmonic force field calculations were to evaluate initial spectroscopic parameters for the minor isotopic species of cyclopropanone and first order vibration-rotation parameters (Mills 1972), see also Sect. 6. Core electrons were kept frozen in MP2, MP3, and CCSD(T) calculations unless “ae” indicates that all electrons were correlated.

4. Spectroscopic properties of cyclopropanone

Cyclopropanone is a planar asymmetric rotor with $\kappa = (2B - A - C)/(A - C) = -0.8801$, somewhat close to the prolate symmetric limit of -1 . Its dipole moment of 4.39 D (Benson et al. 1973) is along the a -inertial axis which is aligned with the CO bond, see Fig. 1. The strongest transitions are R -branch transitions ($\Delta J = +1$) with $\Delta K_a = 0$ and $\Delta K_c = +1$. The Boltzmann peak at 300 K is near 480 GHz. Q -branch transitions with $\Delta K_a = 0$ and $\Delta K_c =$

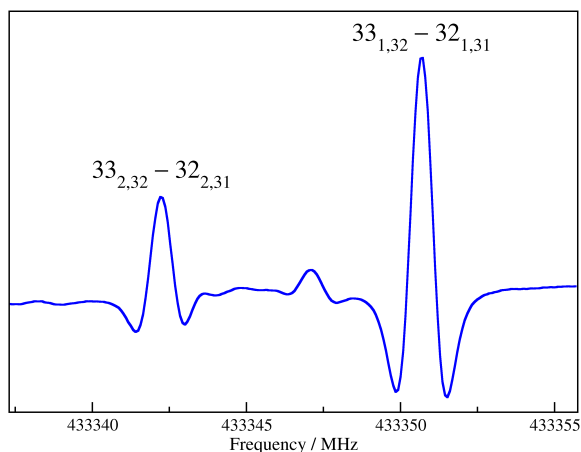


Fig. 2. Section of the submillimeter spectrum of $c\text{-H}_2\text{C}_3\text{O}$. The $K_c = J - 1$ transitions are approaching oblate pairing, that is, the two lines coalesce at somewhat higher J . Also demonstrated is the 1:3 *para* to *ortho* ratio for transitions with K_a being even and odd, respectively; see Sect. 4 for further details.

-1 and transitions with $\Delta K_a = \pm 2$ are much weaker, but can be observed quite readily under favorable circumstances.

Carbon has two stable isotopes with mass numbers 12 and 13 and with terrestrial abundances of 98.89% and 1.11%, respectively (Berglund & Wieser 2011). The respective abundances are 99.76%, 0.04%, and 0.20% for ^{16}O , ^{17}O , and ^{18}O , and 99.98% and $\sim 0.015\%$ for H and D.

The main isotopolog and those with ^{18}O or ^{13}C in the keto group (C1) have C_{2v} symmetry. Spin-statistics caused by the two equivalent H lead to *ortho* and *para* states with a 3:1 intensity ratio, see Fig. 2. The *ortho* states are described by K_a being odd. The doubly deuterated isotopolog has also C_{2v} symmetry, but the *ortho* to *para* ratio is 2:1, and the *ortho* states are described by K_a being even. The effect of substituting ^{13}C at C2 or C3 is the same because the two carbon atoms are structurally equivalent. The corresponding species is thus referred to as $^{13}\text{C}2$ isotopolog. Note that we do not consider isotopologs with more than one ^{13}C . The abundance of the $^{13}\text{C}2$ isotopolog is $\sim 2.2\%$ in a sample of natural isotopic composition. Its symmetry is C_s , as is that of the HD isotopolog. No non-trivial spin-statistics exist in these two isotopologs. The HD isotopolog has a very small b -dipole moment component of ~ 0.21 D as derived from the structure and from quantum-chemical calculations; the corresponding value for the $^{13}\text{C}2$ isotopolog is ~ 0.06 D.

5. Spectroscopic results

Pickett's programs SPCAT and SPFIT (Pickett 1991) were used to calculate and fit the rotational spectra of the cyclopropanone isotopologs. The results of Guillemin et al. (1990) were used for the main species. Too few transition frequencies have been published for the minor isotopic species to determine quartic centrifugal distortion parameters reliably. We evaluated ground state rotational and equilibrium quartic centrifugal distortion parameters for six isotopic species of cyclopropanone at the B3LYP/3a quantum-chemical level; vibrational corrections to centrifugal distortion parameters are, to our knowledge, not available in publicly available quantum-chemical programs. We approximated the experimental value $X_{\text{exp}}^{\text{iso}}$ of an isotopic spectroscopic parameters by scaling the calculated value $X_{\text{calc}}^{\text{iso}}$ with the ratio of the experimental and calculated value $X_{\text{exp}}^{\text{main}}/X_{\text{calc}}^{\text{main}}$ of the main iso-

topolog. These values were used as starting parameters to reproduce the limited sets of transition frequencies of the minor isotopic species. One important aspect in this procedure, and in all of our fitting, was to determine or to float as few parameters as possible to improve the weighted rms of the fit as a useful measure of the quality of the fit. This implies that we searched in each fitting round for the spectroscopic parameter that reduced the weighted rms most and that was useful in the context of parameters already determined or floated in the fit. It was sufficient to float B and C in the cases of the $^{13}\text{C}1$, $^{13}\text{C}2$, and ^{18}O isotopologs of cyclopropanone. One transition of the ^{18}O species, $4_{1,3} - 4_{1,4}$, and two transitions of the $^{13}\text{C}2$ species, $10_{2,8} - 10_{2,9}$ and $15_{3,12} - 15_{3,13}$, had large residuals between the reported experimental frequency and the calculated one that we weighted out these transitions; eventually, they were omitted from the final fits. The reported frequencies were larger than in our final calculations by 0.46 MHz for the line attributed to the ^{18}O species and by 43.51 and 92.56 MHz, respectively, for the two lines assigned to the $^{13}\text{C}2$ isotopolog. We had to float also A to reproduce the transition frequencies of the doubly deuterated isotopolog well. The adjusted rotational parameters of $c\text{-D}_2\text{C}_3\text{O}$ differed somewhat more from the initial parameters than the adjusted B and C values of the other minor isotopic species. We assumed the deviations in the case of $c\text{-HDC}_3\text{O}$ will be roughly half as large as those of $c\text{-D}_2\text{C}_3\text{O}$. We corrected the $c\text{-HDC}_3\text{O}$ accordingly to improve the calculations of this isotopolog for the first searches of rotational transitions.

5.1. The main isotopic species

Our investigations started with measurements of the main isotopic species in the 342–505 GHz region. We targeted the strongest R -branch transitions with $K_a \leq 5$ in a first step, subsequently extending to $K_a = 29$ in few steps. Transitions with $K_a \leq 14$ were found within 0.3 MHz of the initial calculations. The deviations increased rapidly with K_a and exceeded 10 MHz for the highest K_a transitions. We searched then for Q -branch transitions with $\Delta K_a = 0$ and for various types of $\Delta K_a = 2$ transitions, most of them had also $\Delta J = 0$. Later, very limited measurements were carried out in the 160–245 GHz region and then again more extensive ones in the 70–126 GHz region. The $\Delta K_a = \Delta J = 0$ transitions reached $K_a = 8$, and the $\Delta K_a = 2$ transitions extended to $K_a = 5 \leftrightarrow 7$. Whereas the rotational spectrum of cyclopropanone is quite sparse on the level of the strongest lines, it is much richer on the level of the weakest transitions recorded with the consequence that the desired line has an increased chance of being blended with or being close to a usually unassigned line.

In the end, we had recorded 398 different transitions newly which correspond to 311 different frequencies because of 87 unresolved asymmetry doublets. The majority of these doublets are prolate paired transitions, which have the same J and K_a for each pair, as may be expected for an asymmetric rotor somewhat close to the prolate symmetric limit; seven are oblate paired transitions with $K_c = J$ in each case. In addition, we remeasured three transitions already reported by Guillemin et al. (1990). These data were combined with 14 transition frequencies from Benson et al. (1973) and 45 from Guillemin et al. (1990), which corresponded to 51 transitions. Uncertainties of 30 kHz were used for these lines as stated by Guillemin et al. (1990) for their data and commensurate for the data by Benson et al. (1973).

We subjected the transition frequencies initially to fits employing Watson's A reduction, as done previously (Guillemin et al. 1990). We tried out also Watson's S reduction because cy-

Table 1. Present and previous experimental spectroscopic parameters (MHz) of the main isotopolog of cyclopropanone and details on the fits in comparison to values calculated at the B3LYP/3a level.

Parameter	S reduction			A reduction		
	Present	B3LYP/3a ^a	B3LYP/3a ^a	Present	Previous ^b	Parameter
<i>A</i>	32040.68588 (49)	32262.52	32262.52	32240.68387 (51)	32240.734 (25)	<i>A</i>
<i>B</i>	7825.000761 (53)	7823.00	7823.01	7825.045789 (63)	7825.04620 (60)	<i>B</i>
<i>C</i>	6280.728112 (50)	6287.49	6287.48	6287.684168 (62)	6287.68461 (57)	<i>C</i>
$D_K \times 10^3$	46.4328 (91)	44.85	46.47	48.1139 (97)	50.65 (104)	$\Delta_K \times 10^3$
$D_{JK} \times 10^3$	35.87301 (90)	35.27	33.33	33.81184 (90)	33.7882 (50)	$\Delta_{JK} \times 10^3$
$D_J \times 10^6$	1451.833 (24)	1395.	1718.	1794.927 (83)	1793.62 (100)	$\Delta_J \times 10^6$
$d_1 \times 10^6$	-385.4874 (49)	-366.1	21.37	22.2410 (13)	22.156 (15)	$\delta_K \times 10^3$
$d_2 \times 10^6$	-171.7446 (55)	-161.5	366.1	385.546 (20)	385.36 (25)	$\delta_J \times 10^6$
$H_K \times 10^9$		-33.48	-154.9			$\Phi_K \times 10^9$
$H_{KJ} \times 10^9$	363.09 (54)	108.8	153.0	36.1 (22)		$\Phi_{KJ} \times 10^9$
$H_{JK} \times 10^9$	-14.98 (39)	-10.14	75.66	79.55 (83)		$\Phi_{JK} \times 10^9$
$H_J \times 10^{12}$		-226.2	319.0	373. (37)		$\Phi_J \times 10^{12}$
$h_1 \times 10^{12}$		95.67	1245.	1595. (14)		$\phi_K \times 10^9$
$h_2 \times 10^{12}$	276.4 (36)	272.6	43.33	40.97 (85)		$\phi_{JK} \times 10^9$
$h_3 \times 10^{12}$	193.0 (12)	151.1	246.7	201. (11)		$\phi_J \times 10^{12}$
J_{\max}	48			48	27	
$K_{a,\max}$	29			29	12	
No. transitions	463			463		
No. frequencies	370			370	59	
rms	0.0248			0.0243	0.028	
rms (new)^c	0.0236			0.0229		
rms (B)^c	0.0293			0.0292		
rms (G)^c	0.0312			0.0310		
wrms ^d	0.972			0.921		
wrms (new)^c	0.961			0.901		
wrms (B)^c	0.978			0.972		
wrms (G)^c	1.041			1.034		

Notes. Watson's *S* and *A* reductions were used in the representation *I'*. Numbers in parentheses are one standard deviation in units of the least significant figures. Empty fields indicate parameters not used in the fit. ^(a) Ground state rotational and equilibrium centrifugal distortion parameters. ^(b) Guillemin et al. (1990). ^(c) **The labels (new), (B), and (G) refer to our new data, those from Benson et al. (1973), and from Guillemin et al. (1990).** ^(d) Weighted rms, unit-less.

clopropanone is quite close to the prolate symmetric limit, in which case the *S* reduction is usually preferable. As can be seen in Table 1, we required an almost complete parameter set up to sixth order in the *A* reduction, only Φ_K was not used in the fit. Two fewer parameters were used in the *S* reduction, albeit with a slightly larger wrms of 0.972 compared to 0.921. Nevertheless, we decided to view the *S* reduced fit as the preferred one. Trial fits with Φ_K or H_K , H_J , and h_1 from B3LYP/3a calculations added to the fit as fixed parameters did not improve the quality of the fits and resulted in changes of the remaining spectroscopic parameters roughly corresponding to their uncertainties. Moreover, we were uncertain concerning the reliability of the quantum-chemically calculated sextic distortion parameters, see also Sect. 7.1. Therefore, these parameters were omitted from the final fits. The quantum-chemically calculated spectroscopic parameters are given in Table 1 for comparison purpose along with the parameters from Guillemin et al. (1990). **We also provide rms values for the whole data set and for the individual sources for completeness reason. The rms is meaningful if only one uncertainty was used in all instances or if the uncertainties differ only by a factor of a few. In the present case,**

the uncertainties differ by around a factor of 10. In this and similar cases, the rms is dominated by the lines with large residuals.

5.2. The ¹³C1, ¹³C2, and ¹⁸O isotopologs

We began our investigations of the minor isotopologs of cyclopropanone containing one ¹³C or ¹⁸O in the 160–245 GHz region searching for the stronger *R*-branch transitions first with $K_a \leq 2$ and then up to $K_a = 5$. Additional measurements were carried out in the 70–126 GHz region, in which we recorded *R*-branch transitions up to $K_a = 7$ and several $\Delta K_a = \Delta J = 0$ transitions for the two isotopomers with one ¹³C. The extent of measured lines was more limited for the ¹⁸O because of its lesser abundance.

The final line lists of the ¹³C1, ¹³C2, and ¹⁸O isotopologs consist of 104, 95, and 48 different and new transition frequencies, respectively, in addition to the small number of previously reported lines (Benson et al. 1973), for which uncertainties of 70 kHz were assigned. The resulting sets of spectroscopic parameters, determined as described at the beginning of this sec-

Table 2. Spectroscopic parameters (MHz) from a minimum parameter set, a maximum parameter set, and initial parameters along with details on the fits of the $^{13}\text{C}1$, $^{13}\text{C}2$, and ^{18}O isotopologs of cyclopropanone.

Parameter	Minimum	Maximum	Initial
$^{13}\text{C}1$ isotopolog			
A	32040.141 (4)	32040.176 (18)	32040.226
B	7816.5529 (2)	7816.5525 (2)	7816.565
C	6275.2893 (2)	6275.2894 (2)	6275.289
$D_K \times 10^3$	46.61	49.9 (26)	46.61
$D_{JK} \times 10^3$	35.636 (6)	35.634 (8)	35.659
$D_J \times 10^6$	1453.62 (34)	1452.67 (71)	1454.9
$d_1 \times 10^6$	-385.54	-384.74 (29)	-385.54
$d_2 \times 10^6$	-170.65	-170.99 (38)	-170.65
J_{\max}	21 (15)	21 (15)	
$K_{a,\max}$	7 (3)	7 (3)	
No. trans.	115 (6,-0) ^c	115 (6,-0) ^a	
No. freqs.	110 (6,-0) ^c	110 (6,-0) ^a	
rms	0.0271	0.0186	
wrms ^b	0.782	0.722	
$^{13}\text{C}2$ isotopolog			
A	31174.389 (6)	31173.391 (6)	31175.000
B	7709.4761 (1)	7709.4759 (2)	7709.598
C	6172.7465 (1)	6172.7466 (2)	6172.943
$D_K \times 10^3$	44.80 (41)	44.36 (47)	42.79
$D_{JK} \times 10^3$	34.656	34.654 (7)	34.656
$D_J \times 10^6$	1402.36 (33)	1402.22 (35)	1403.8
$d_1 \times 10^6$	-376.82	-376.55 (13)	-376.82
$d_2 \times 10^6$	-169.59 (15)	-169.57 (18)	-169.63
J_{\max}	30 (6)	30 (6)	
$K_{a,\max}$	7 (1)	7 (1)	
No. trans.	106 (5,-2) ^c	106 (5,-2) ^a	
No. freqs.	100 (5,-2) ^c	100 (5,-2) ^a	
rms	0.0184	0.0180	
wrms ^b	0.796	0.766	
^{18}O isotopolog			
A	32040.339	32240.323 (53)	32040.339
B	7344.8771 (3)	7344.8759 (7)	7344.714
C	5967.5319 (3)	5967.5326 (6)	5967.034
$D_K \times 10^3$	49.85	49.85	49.85
$D_{JK} \times 10^3$	32.611	32.594 (17)	32.611
$D_J \times 10^6$	1308.6	1307.9 (12)	1308.6
$d_1 \times 10^6$	-324.81	-322.8 (13)	-324.81
$d_2 \times 10^6$	-138.10	-136.8 (10)	-138.10
J_{\max}	19 (14)	19 (14)	
$K_{a,\max}$	5 (3)	5 (3)	
No. trans.	61 (10,-1) ^c	61 (10,-1) ^a	
No. freqs.	58 (10,-1) ^c	58 (10,-1) ^a	
rms	0.0545	0.0525	
wrms ^b	0.871	0.801	

Notes. Watson's S reduction was used in the representation I' . Numbers in parentheses of parameters are one standard deviation in units of the least significant figures. Numbers in parentheses associated with numbers of quantum numbers, transitions, and lines, respectively, refer to data from the previous study (Benson et al. 1973). Parameters without uncertainties were estimated and kept fixed in the analyses, see Sect. 5. ^(a) With omitted lines after the comma, see Sect. 5. ^(b) Weighted rms, unit-less.

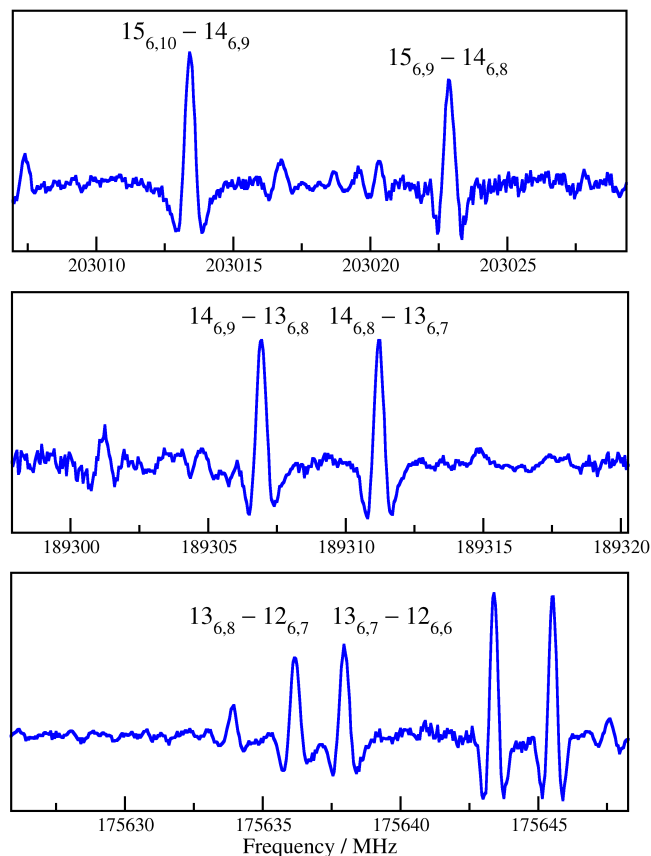


Fig. 3. Section of the millimeter spectrum of cyclopropanone highly enriched in deuterium. Transitions with small, but rapidly increasing asymmetry splitting are shown for $K_a = 6$ of $c\text{-HDC}_3\text{O}$. These transitions were the first which we assigned because of their easily recognizable patterns.

tion, had A and two respectively three quartic distortion parameters floated in addition to B and C for $^{13}\text{C}1$ and $^{13}\text{C}2$. It was sufficient to float only B and C in the case of the ^{18}O isotopolog. The parameter values, their uncertainties, and additional details on the fits are presented in Table 2 as minimum parameter sets which are the preferred parameter sets. We also tested how many parameters can be determined with sufficient significance. These were all quartic centrifugal distortion parameters for the isotopomers with one ^{13}C and all but ΔD_K for the ^{18}O isotopolog. The resulting values are given as maximum parameter sets in the same table along with the initial parameters whose derivation was also described at the beginning of this section.

5.3. The singly and doubly deuterated isotopic species

Our procedure for studying the rotational spectrum of the D_2 isotopolog was very similar to that for the minor isotopic species described in the previous subsection. The use of a sample highly enriched in deuterium made it possible to record considerably more transitions extending to higher quantum numbers. The spectral recordings were line richer than those of the sample in natural isotopic composition because of the presence of lines caused by the HD species and even some of the main species. In addition, we identified lines of traces of CH_2Cl_2 which was used as a solvent in the course of the preparation of the deuterated sample and which was difficult to remove completely.

The R -branch transitions with $\Delta K_a = 0$ were recorded up to $K_a = 9$, transitions with $\Delta K_a = \Delta J = 0$ up to 2, and those with $\Delta K_a = 2$ up to $K_a = 5 \leftarrow 3$.

We employed a different strategy to search for transitions of the HD isotopolog because no previous data existed. A pattern of two or more transitions is obviously more decisive than a single line. The best candidates are nearly prolate or nearly oblate paired R -branch transitions because the small asymmetry splitting changes rapidly with J . The asymmetry splitting of the $K_c = J$ nearly oblate paired transitions were deemed to be too large in the 160–245 GHz region. As can be seen in Fig. 3, the $K_a = 6$ nearly prolate paired transitions were suited very well, even though they were considerably weaker. The measured asymmetry splittings of about 1.8, 4.4, and 9.5 MHz for $J'' = 12$ to 14 compared very well with the calculated splittings. We searched for R -branch transitions with equal or lower K_a with an improved calculation of the rotational spectrum. Subsequently, we sought Q -branch transitions with $\Delta K_a = 0$ and 2, respectively. Our line list reached $K_a = 3$ in the first case and $K_a = 3 \leftarrow 1$ in the second case of these weaker transitions.

We did not target any b -type transitions of c -HDC₃O as these were calculated to be even weaker than many of the $\Delta K_a = 2$ transitions. Some b -type transitions were covered by accident; even much longer integration times may not have helped because the amount of lines with similar or larger intensities were so large that it would be difficult to identify unblended lines unambiguously. In addition, it is important to note that $\Delta K_a = 1$ transitions carry less information on the purely K dependent parameters than do those with $\Delta K_a = 2$ at similar values of K_a .

The minimum parameter sets for both deuterated isotopologs were determined as described above. Interestingly, we obtained a satisfactory fit for 172 different frequencies of c -D₂C₃O after floating only two of the five quartic centrifugal distortion parameters whereas we required four for 126 different frequencies of c -HDC₃O; this is probably a consequence of the choice of the covered transitions. In the fit of c -D₂C₃O with the full parameter set, ΔD_J and ΔD_{JK} improved the wrms by similar amounts. The parameter values, their uncertainties, and additional details on the fits are presented in Table 3.

6. Structural parameters of cyclopropenone

Several methods exist to derive structural parameters of a molecule from its moments of inertia, which are inversely proportional to the rotational parameters. The results depend on the model to a varying degree, and some methods do not even yield the same result for different data sets in theory. Data of different isotopologs are required for molecules with three or more symmetry-inequivalent atoms; it is usually desirable to have each symmetry-inequivalent atom substituted once to be able to obtain reliable structural parameters.

The ground state effective (or r_0) structure is the most straightforward model in which the structural parameters are fit to the ground state moments of inertia. The ground state values are usually the ones determined first, and often they are the only ones. The ground state moments of inertia contain vibrational contributions from the zero-point vibrations, causing the r_0 structure to be one of the less meaningful structure models with sometimes relatively large changes with isotopic data set.

The differences in the moments of inertia caused by the substitution of one or more symmetry-inequivalent atoms can be used to determine the Cartesian coordinates of these atoms (Kraitchman 1953; Costain 1958). The resulting substitution (or r_s) structure reduces the effects of vibrational contributions to

Table 3. Spectroscopic parameters (MHz) from a minimum parameter set, a full parameter set, and initial parameters along with details on the fits of the mono and doubly deuterated isotopologs of cyclopropenone.

Parameter	Minimum	Full	Initial
HD isotopolog			
A	28049.092 (3)	28049.090 (4)	28035.946
B	7510.3156 (1)	7510.3156 (1)	7509.008
C	5916.1823 (1)	5916.1823 (1)	5915.416
$D_K \times 10^3$	46.16	45.95 (33)	46.16
$D_{JK} \times 10^3$	29.541 (3)	29.541 (3)	29.509
$D_J \times 10^6$	1347.93 (15)	1347.99 (18)	1349.3
$d_1 \times 10^6$	-412.68 (8)	-412.71 (9)	-414.44
$d_2 \times 10^6$	-180.56 (68)	-180.54 (72)	-181.29
J_{\max}	20 (0)	20 (0)	
$K_{a,\max}$	7 (0)	7 (0)	
No. trans.	130 (0)	130 (0)	
No. freqs.	126 (0)	126 (0)	
rms	0.0126	0.0122	
wrms ^a	0.817	0.815	
D ₂ isotopolog			
A	24535.524 (1)	24535.521 (3)	24514.520
B	7254.9417 (1)	7254.9422 (1)	7252.557
C	5591.7853 (1)	5591.7855 (1)	5590.549
$D_K \times 10^3$	30.37	30.20 (11)	30.37
$D_{JK} \times 10^3$	27.185	27.189 (1)	27.185
$D_J \times 10^6$	1179.79	1180.35 (13)	1179.8
$d_1 \times 10^6$	-410.13 (10)	-410.31 (11)	-412.33
$d_2 \times 10^6$	-199.06 (4)	-199.10 (5)	-200.75
J_{\max}	24 (10)	24 (10)	
$K_{a,\max}$	9 (2)	9 (2)	
No. trans.	189 (10)	189 (10)	
No. freqs.	172 (10)	172 (10)	
rms	0.0222	0.0214	
wrms ^a	0.917	0.810	

Notes. Watson's S reduction was used in the representation I' . Numbers in parentheses of parameters are one standard deviation in units of the least significant figures. Numbers in parentheses associated with numbers of quantum numbers, transitions, and lines, respectively, refer to data from the previous study (Benson et al. 1973). Parameters without uncertainties were estimated and kept fixed in the analyses, see Sect. 5.
(^a) Weighted rms, unit-less.

the ground state moments of inertia, albeit to a varying degree. The r_s structure is equivalent to $r_{\Delta I}$, the structure that is obtained by fitting structural parameters to the differences of the moments of inertia (Rudolph 1991). This structure is, in turn, equivalent to the $r_{I,\epsilon}$ structure, in which vibrational contributions ϵ_i to the ground state moments of inertia, that is $I_{ii,0} = I_{ii,e} + \epsilon_i$, with $i = a, b, c$, are assumed to be equal for different isotopologs of a given molecule. The advantage of taking ϵ_i into account explicitly is that rotational parameters of isotopic species to be studied can be estimated much better, in particular for atoms with more than two isotopes or for multiply substituted isotopologs (Epple & Rudolph 1992; Müller & Gerry 1994; Müller et al. 2019), if residuals of known isotopologs can be transferred to the values of the desired isotopolog. In the case of H₂CS, Müller et al. (2019)

Table 4. Ground state rotational parameters $B_{i,0}$ of cyclopropenone isotopic species, vibrational corrections $\Delta B_{i,v}^a$, resulting semi-empirical equilibrium rotational parameters $B_{i,e}^{\text{SE}}$, and inertia defects Δ .^b

Species	B_i/Δ	$B_{i,0}$	B3LYP		MP2		ae-MP2	
			$\Delta B_{i,v}$	$B_{i,e}^{\text{SE}}$	$\Delta B_{i,v}$	$B_{i,e}^{\text{SE}}$	$\Delta B_{i,v}$	$B_{i,e}^{\text{SE}}$
main	A	32040.686	167.049	32207.735	179.586	32220.272	183.294	32223.980
	B	7825.001	33.674	7858.675	34.377	7859.378	34.577	7859.578
	C	6280.728	36.969	6317.697	37.689	6318.417	37.999	6318.727
	Δ	0.1068		-0.00547		-0.00273		-0.00321
¹³ C1	A	32040.141	167.513	32207.654	180.110	32220.251	183.804	32223.945
	B	7816.553	33.050	7849.603	33.778	7850.331	33.969	7850.522
	C	6275.289	36.543	6311.832	37.281	6312.570	37.584	6312.873
	Δ	0.1065		-0.00550		-0.00276		-0.00324
¹³ C2	A	31174.389	161.272	31335.661	173.586	31347.975	177.251	31351.640
	B	7709.476	32.969	7742.445	33.660	7743.136	33.863	7743.339
	C	6172.746	36.126	6208.872	36.842	6209.588	37.155	6209.901
	Δ	0.1083		-0.00548		-0.00270		-0.00321
¹⁸ O	A	32040.339	167.399	32207.738	180.001	32220.340	183.743	32224.082
	B	7344.877	31.126	7376.003	31.751	7376.628	31.941	7376.818
	C	5967.532	34.415	6001.947	35.072	6002.604	35.363	6002.895
	Δ	0.1079		-0.00537		-0.00264		-0.00314
HD	A	28049.092	130.214	28179.306	137.620	28186.712	140.330	28189.422
	B	7510.316	31.968	7542.284	32.521	7542.837	32.719	7543.035
	C	5916.182	34.032	5950.214	34.480	5950.662	34.764	5950.946
	Δ	0.1142		-0.00590		-0.00267		-0.00325
D ₂	A	24535.524	98.171	24633.695	102.770	24638.294	105.086	24640.610
	B	7254.942	31.074	7286.016	31.600	7286.542	31.729	7286.671
	C	5591.785	31.521	5623.306	31.843	5623.628	32.081	5623.866
	Δ	0.1210		-0.00641		-0.00272		-0.00337

Notes. ^(a) $\Delta B_{i,v} = \sum_j \alpha_j^B / 2$ calculated by different quantum-chemical means as detailed in Sect. 3. ^(b) All numbers in units of MHz, except Δ in units of $\text{amu} \text{ \AA}^2$.

extrapolated the residuals of H₂C³²S, H₂C³³S, and H₂C³⁴S to H₂C³⁶S, and those of H₂C³²S, H₂C³⁴S, and H₂¹³CS to H₂¹³C³⁴S.

The equilibrium (or r_e) structure of a molecule in the potential minimum is the most meaningful structure. It is, however, also the most elusive structure because not only data of more than one isotopolog are needed for molecules with three or more symmetry-inequivalent atoms, but for each isotopolog we require the knowledge of several vibration-rotation parameters according to

$$B_e = B_0 + \frac{1}{2} \sum_j \alpha_j^B - \frac{1}{4} \sum_{j \leq k} \gamma_{jk}^B - \dots \quad (1)$$

in order to evaluate the equilibrium parameter B_e from the ground state value B_0 . Here, the α_j^B are first order vibrational corrections, the γ_{jk}^B are second order vibrational corrections, and so on. Equivalent formulations hold for A_e and C_e . An attractive and lately very common approach is to calculate $\sum_j \alpha_j^B / 2$ by quantum-chemical means to derive semi-empirical equilibrium rotational parameters $B_{i,e}$ from the experimental ground state values (Stanton et al. 1998). Second and higher order vibrational contributions are neglected. Numerous quantum-chemical programs are available to carry out such calculations; examples have been mentioned in Sect. 3.

We used B3LYP, MP2, and ae-MP2 calculations with a triple zeta basis set to evaluate the first order vibrational corrections for isotopologs of cyclopropenone which are summarized in Table 4 together with ground state values and the resulting semi-empirical equilibrium values. The inertia defect $\Delta = I_{cc} - I_{bb} - I_{aa}$ is also given for each set of rotational parameters.

We employed the RU111J program (Rudolph 1995) to derive semi-empirical equilibrium structural parameters r_e^{SE} for each of the three quantum-chemical calculations. The results are given in Table 5 together with structural parameters purely from quantum-chemical calculations and with the r_s parameters from Benson et al. (1973). The differences between the r_s parameters and our r_e^{SE} parameters turned out to be larger than expected and will be discussed in detail in Sect. 7.2. We calculated subsequently $r_{I,\epsilon}$ structures, which are equivalent to r_s structures as mentioned above, in order to evaluate the dependence of the resulting parameters on diverse input data. The first set of input data were our present rotational data from six isotopic species as summarized in Table 4. The second set employed our starting values as described in Sect. 5. The third set were the rotational parameters from Benson et al. (1973), but without A(¹³C2), as it deviated by 61 MHz from the value of our preferred fit. The results of these structure fits are also given (in reverse order) in Table 5.

Table 5. Quantum-chemical and experimental bond lengths (pm) and bond angles (deg) of cyclopropanone.

Method ^a	$r(\text{CO})$	$r(\text{C}-\text{C})$	$r(\text{C}=\text{C})^b$	$r(\text{CH})$	$\angle(\text{OCC})$	$\angle(\text{C3C1C2})^b$	$\angle(\text{C1C2H})$
B3LYP/3a	120.157	142.672	133.964	108.054	151.999	56.001	153.841
B3LYP/4a	120.000	142.626	133.894	108.005	152.005	55.989	153.852
B3LYP/4aC	119.989	142.613	133.887	108.018	152.004	55.991	153.856
MP2/3a	120.681	143.399	135.270	107.970	151.858	56.284	154.166
MP2/4a	120.388	143.046	134.907	107.850	151.865	56.270	154.150
MP2/5a	120.313	142.962	134.815	107.817	151.868	56.264	154.142
ae-MP2/3aC	120.395	142.885	134.752	107.822	151.866	56.268	154.148
ae-MP2/4aC	120.140	142.612	134.496	107.689	151.865	56.270	154.139
ae-MP2/5aC	120.078	142.531	134.408	107.655	151.868	56.264	154.132
MP3/3a	119.628	142.810	134.383	107.698	151.934	56.133	153.478
ae-MP3/3aC	119.355	142.333	133.908	107.556	151.940	56.121	153.460
CCSD(T)/3a	120.684	143.735	135.308	108.155	151.921	56.158	153.739
CCSD(T)/4a	120.346	143.347	134.912	108.030	151.928	56.144	153.731
ae-CCSD(T)/3aC	120.404	143.267	134.832	108.010	151.929	56.142	153.724
r_s^c	121.2 (2)	141.2 (3)	130.2 (3)	109.7 (3)		54.9 (7)	152.5 (5)
$r_{I,\epsilon}(\text{old})^d$	120.29 (36)	143.18 (46)	134.90 (85)	107.82 (31)	151.89 (22)	56.21 (45)	153.91 (41)
$r_{I,\epsilon}(\text{old})^e$	120.47 (30)	142.88 (38)	134.84 (38)	107.88 (16)	151.84 (12)	56.31 (23)	154.02 (22)
$r_{I,\epsilon}(\text{new})^f$	120.44 (28)	142.91 (35)	134.73 (14)	107.90 (9)	151.88 (8)	56.24 (16)	153.95 (14)
$r_e^{\text{SE}}(\text{B3LYP})^g$	120.04 (21)	142.91 (17)	134.532 (6)	107.77 (4)	151.92 (4)	56.16 (7)	153.74 (6)
$r_e^{\text{SE}}(\text{MP2})^g$	120.05 (10)	142.88 (8)	134.480 (4)	107.84 (2)	151.93 (2)	56.15 (3)	153.73 (3)
$r_e^{\text{SE}}(\text{ae-MP2})^g$	120.05 (12)	142.87 (10)	134.468 (4)	107.85 (2)	151.93 (2)	56.14 (4)	153.73 (3)

Notes. All values from this work unless indicated otherwise. Numbers in parentheses are one standard deviation in units of the least significant figures. ^(a) Quantum-chemical calculations as detailed in Sect. 3; structural parameter determinations as described in Sect. 6. ^(b) Derived parameter in present calculations. ^(c) Benson et al. (1973); structural parameters derived from substitution coordinates; $\angle(\text{C1C2H})$ calculated from $\angle(\text{C2C3H})$ and $\angle(\text{C3C1C2})$. ^(d) This work; rotational parameters from Benson et al. (1973), but $A(^{13}\text{C2})$ omitted; see also Sects. 6. ^(e) This work; rotational parameter derived as described in Sect. 5 using data from Benson et al. (1973) and Guillemin et al. (1990). ^(f) This work; rotational parameters from this work. ^(g) Quantum-chemical method in parentheses as detailed in Sect. 6; see also Table 4.

7. Discussion

7.1. Spectroscopic parameters

As can be seen in Table 1, the J and K_a quantum number ranges and also the number of different transition frequencies of the main isotopolog of cyclopropanone have been greatly increased in the course of the present investigation with respect to the previous study (Guillemin et al. 1990). The previous spectroscopic parameters agree well with ours in the A reduction taking into account the uncertainties in that work. The B3LYP/3a quantum-chemically calculated ground state rotational and equilibrium quartic centrifugal distortion parameters agree quite well with our experimental values in both reductions. The comparison of the sextic centrifugal distortion parameters is more mixed as far as experimental values are available; trial fits showed that the experimental values are only slightly affected by the absence of three and one sextic parameter in the S and A reduction, respectively. This shows that the deviations seen in particular in H_{KJ} and the corresponding Φ_{KJ} are not mainly caused by the omission of the three or one parameter. Moreover, a trial fit with h_1 in the fit yielded a value of $19 \pm 10 \mu\text{Hz}$, not compatible with the calculated $96 \mu\text{Hz}$.

Our final fit in the S reduction has two parameters less than the one in the A reduction at the expense of a slightly larger wrms. We consider this improvement to be sufficient to favor the S reduction. Additional reasons for preferring the S reduction are that it is more versatile than the A reduction as the latter can exhibit convergence problems for molecules close to the prolate or

oblate symmetric limit. Moreover, Watson (1977) recommended to use the S reduction because such fits yield smaller correlation coefficients. This conclusion was recently reemphasized in an extensive study of the rotational spectra of SO^{18}O and S^{18}O_2 in their lowest two and three vibrational states, respectively, with detailed analyses of the fits (Margulès et al. 2020).

Our spectroscopic parameters for the $^{13}\text{C1}$, $^{13}\text{C2}$, and ^{18}O isotopologs in Table 2 agree very well with our initial values both for the minimum and maximum parameter sets. The agreement is good in the cases of the deuterated isotopologs, as can be seen in Table 3. The parameter D_K from the full parameter sets of both deuterated isotopologs agrees very well with the initial values, which may indicate that the small changes in D_K seen for the isotopomers containing one ^{13}C may, nevertheless, be too large.

The initial spectroscopic parameters of all minor isotopic species were derived from quantum-chemically calculated ones scaled with the respective ratios between experimental and calculated value of the main species as described in slightly more detail at the beginning of Sect. 5. Such scaling was used, for example, to evaluate some sextic centrifugal distortion parameters of two minor isotopologs of TiO_2 (Kania et al. 2011). Cazzoli et al. (2014) demonstrated in a study of the rotational spectrum of H_2^{36}S that such scaling works very well even for heavy atom substitutions of relatively light molecules such as H_2S . Higher level quantum-chemical calculations, as employed by Cazzoli et al. (2014), may lead to better starting values than the lower level calculations used here. However, higher level calculations are computationally more demanding, in particular for somewhat

larger molecules. Moreover, Morgan et al. (2018) have shown that considerable computational effort is necessary to obtain systematically converged very good results even for the fairly small molecule formaldehyde, H_2CO . The quality of the scaling of centrifugal distortion parameters may be limited in addition by the lack of vibrational corrections. Quartic and sextic equilibrium centrifugal distortion parameters can be calculated with several quantum-chemical programs, but the derivation of vibrational corrections is, to the best of our knowledge, not possible with any publicly available program.

Scaling of quantum-chemically derived distortion parameters should be better than scaling by appropriate powers of the ratios of $2A - B - C$, $B + C$, and $B - C$, as done, for example, in the recent case of isotopic H_2CS (Müller et al. 2019). This type of scaling works usually quite well for heavy atom substitutions, but less so for H to D substitutions, in particular for molecules with few atoms. Fixing parameters of minor isotopologs, which cannot be determined sufficiently well, to values from the main isotopic species work usually less well, but is in most cases better than fixing such parameters to zero.

We may ask ourselves what are the advantages or disadvantages of our minimum parameter fits compared to our maximum parameter fits. Increasing the parameter set beyond the optimum increases the uncertainties, usually the correlation among the parameters, and affects the parameter values frequently outside the initial uncertainties. Therefore, transition frequencies calculated with fewer parameters are often better in cases of interpolation or modest extrapolation compared to values from a larger parameter set. On the other hand, calculated uncertainties become too optimistic sooner upon extrapolation for a smaller parameter set. Extrapolation in J from our present data should be reasonable to two times the upper frequency limit for the strong R -branch transition which is ~ 1.0 THz for the main isotopolog and 450 to 500 GHz for the minor isotopologs. Extrapolation in K_a is much more limited.

The ground state inertia defects in Table 4 are relatively small and positive, as is common for planar molecules with small out-of-plane vibrational amplitudes. The semi-empirical equilibrium inertia defects, obtained from the ground state rotational constants after subtracting off the first order vibrational corrections, are much smaller in magnitude and negative, which is also very common.

7.2. Structural parameters

Our semi-empirical equilibrium structural parameters in Table 5 are largely very similar among the three different sets. The CO bond length has fairly large uncertainties, but displays almost no scatter; the C=C bond shows, in contrast, more pronounced, though still modest variations, which are only a few times the combined uncertainties for the parameters employing B3LYP and ae-MP2 corrections. The CH bond varies about equally much, albeit has larger uncertainties than the C=C bond.

The previously published r_s structure (Benson et al. 1973) agrees, at best, reasonably well with our r_e^{SE} structures; the C=C bond length difference is, with more than 4 pm, particularly large. We calculated $r_{l,\epsilon}$ structures which are equivalent to the r_s structure (Rudolph 1991). Using our ground state rotational data of six isotopologs, as summarized in Table 4, we obtained structural parameters close to our r_e^{SE} values, the largest difference of 0.4 pm occurs in the CO bond length and is even within the combined uncertainties. The initial parameters of five isotopic species, as derived in Sect. 5, yielded essentially the same parameters, the main differences are larger uncertainties in some

parameters, most likely caused by the absence of data of the HD isotopolog. And even the fit with values from Benson et al. (1973) yields results quite similar to the other two $r_{l,\epsilon}$ fits. The deviation of the r_s structure parameters appears thus to be caused by the difference of 61 MHz in $A(^{13}\text{C}_2)$ which is mainly caused by two lines falsely attributed to the $^{13}\text{C}_2$ isotopolog, see also Sect. 5.

The quantum-chemical calculations in Table 5 show very small changes with basis set and also rather small changes between the different methods. The bond lengths display the usual shortening upon increasing basis set size and upon correlation of all electrons as far as applicable. The bond lengths differ substantially among the different methods. The B3LYP parameters show little change with basis set size and agree quite well with our r_e^{SE} values. The largest deviation is seen for the C=C bond length, which is too short by about 0.5 pm. The C–C bond length is also too short, but by smaller amounts, whereas the CO and CH bonds were calculated slightly too long. The MP2/5a and ae-MP2/5aC structures agree between well and very well with our r_e^{SE} structure, the MP2/5a values are slightly closer for the C–C and CH bonds, whereas the ae-MP2/5aC are slightly closer for the other two bond lengths. Calculations using MP3 are sometimes better than those with MP2, but usually worse than those with CCSD(T). In the case of cyclopropanone, already some bond lengths are too short at the MP3/3a level, even more so at ae-MP3/3aC level. Bond lengths at the CCSD(T)/3a level are rather long. The effects of correlating all electrons compared to those with frozen core are similar to those of MP2 calculations employing basis sets of triple zeta quality. If we assume the relative differences are the same for basis sets of quadruple zeta quality, we can estimate the following ae-CCSD(T)/4aC bond lengths: $r(\text{CO}) \approx 120.10$ pm, $r(\text{C–C}) \approx 142.95$ pm, $r(\text{C=C}) \approx 134.53$ pm, and $r(\text{CH}) \approx 108.00$ pm, all very close to our r_e^{SE} values; this behavior is common for ae-CCSD(T)/4aC calculations.

Structural parameters of cyclopropanone are compared with those of other molecules in Table 6. Cyclopropenylidene is suited best for a comparison as it is basically cyclopropanone without the O atom. The O atom withdraws electron density from the cyclopropenylidene rest, causing an elongation of all bond lengths; the effect is smallest for the distant CH bond. Formaldehyde is probably the prototypical molecule with a CO double bond. Its CO bond is only slightly longer than that of $c\text{-H}_2\text{C}_3\text{O}$. The C=C bond lengths of $c\text{-H}_2\text{C}_3\text{O}$ and $c\text{-C}_3\text{H}_2$ are essentially equal to the one in C_2H_4 , and thus typical CC double bonds. The C–C bonds of both cyclic molecules, however, are much shorter than that of ethane, whose C–C bond can probably be viewed as a prototypical CC single bond. In fact, these bonds are only slightly longer than the aromatic CC bonds in benzene. Finally, the CH bond lengths in $c\text{-H}_2\text{C}_3\text{O}$ and $c\text{-C}_3\text{H}_2$ are substantially shorter than in C_2H_4 , but much longer than ~ 106.2 pm in acetylene (Liévin et al. 2011; Tamassia et al. 2016). All this reflects the aromatic character of cyclopropanone (Anonymous 1983; Wang et al. 2011) and cyclopropenylidene from a structural point of view.

8. Conclusion and outlook

Our data for five minor isotopic species of cyclopropanone are sufficient for astronomical searches in cold molecular clouds even without any extrapolation as the Boltzmann peak at 10 K is at ~ 95 GHz. Extrapolation of the data in J should be reasonable up to 450 or 500 GHz. Such extrapolations should be possible up to 1 THz for the main isotopic species, which is sufficient even

Table 6. Equilibrium bond lengths (pm) and selected bond angles (deg) of cyclopropenone in comparison to related molecules.

Molecule	$r(\text{CO})$	$r(\text{C}-\text{C})$	$r(\text{C}=\text{C})$	$r(\text{CH})$	$\angle(\text{C3C1C2})$	$\angle(\text{C1C2H})$
$c\text{-H}_2\text{C}_3\text{O}^a$	120.05 (12)	142.87 (10)	134.468 (4)	107.85 (2)	56.14 (4)	153.73 (3)
$c\text{-C}_3\text{H}_2^b$		141.72 (1)	132.19	107.51 (2)	55.60 (1)	147.78 (3)
H_2CO^c	120.461 (19)			110.046 (16)		
C_2H_6^d		152.2 (2)		108.9 (1)		
$c\text{-C}_6\text{H}_6^e$		139.14 (10)		108.02 (20)		
C_2H_4^f			133.07 (3)	108.09 (3)		

Notes. Numbers in parentheses are one standard deviation in units of the least significant figures. If no uncertainties are given, none were published. ^(a) This work, r_e^{SE} with ae-MP2 corrections. ^(b) Spezzano et al. (2012); r_e^{SE} , ae-CCSD(T)/4C values; $r(\text{C}=\text{C})$ calculated from $r(\text{C}-\text{C})$ and $\angle(\text{C3C1C2})$. ^(c) Lohilahti (2006); experimental r_e values. ^(d) Harmony (1990); r_m^{SE} values according to the second set of data; see Harmony & Taylor (1986) for the definition of this structure model. ^(e) Gauss & Stanton (2000); r_e^{SE} at the CCSD(T)/4 level. ^(f) Martin & Taylor (1996); r_e values from CCSD(T) calculations extrapolated to infinitely large basis set with ae corrections and empirical adjustments.

for rotational temperatures around 300 K. We assume, however, that rotational temperatures of $c\text{-H}_2\text{C}_3\text{O}$ in warmer sources will be closer to 100 K, based on findings for propanal, propenal and propene in IRAS 16293–2422 B (Lykke et al. 2017; Manigand et al. 2021).

Dedicated searches will probably be necessary to detect minor isotopologs of cyclopropenone in space. $c\text{-HDC}_3\text{O}$ is the most promising one to be found in cold molecular clouds. One of the most sensitive molecular line surveys of such sources is the one by Cernicharo et al. (2020) between 31.4 and 50.3 GHz carried out with the Yebes 40 m radio telescope with additional data from the 3 mm region taken earlier with the IRAM 30 m dish. Cernicharo et al. (2020) report the detection of HC_3O^+ and investigated the chemistry of oxygen-containing molecules in TMC-1. They derived a column density of $(4.0 \pm 0.2) \times 10^{11} \text{ cm}^{-2}$ for $c\text{-H}_2\text{C}_3\text{O}$. The most constraining transition of $c\text{-HDC}_3\text{O}$ in that survey is the $3_{13} - 2_{12}$ transition at 37833.721 MHz. The 3σ upper limit to its intensity in brightness temperature is ~ 2.6 mK (with corrections for beam dilution and beam efficiency); the corresponding intensity of the $3_{13} - 2_{12}$ *ortho* transition of $c\text{-H}_2\text{C}_3\text{O}$ is 42 mK, yielding a 3σ column density ratio of > 16 for $c\text{-H}_2\text{C}_3\text{O}$ to $c\text{-HDC}_3\text{O}$ (J. Cernicharo, private communication to HSPM, Nov./Dec. 2020). This is less constraining than the corresponding ratios of, for example, ~ 34 and ~ 25 found for $c\text{-C}_3\text{H}_2$ to $c\text{-C}_3\text{HD}$ (Bell et al. 1986) and $l\text{-C}_3\text{H}_2$ to $l\text{-C}_3\text{HD}$ (Spezzano et al. 2016), respectively, in TMC-1. There are, however, sources with higher degrees of deuteration that may be considered if their column densities of $c\text{-H}_2\text{C}_3\text{O}$ are sufficiently large. A search for the cyclopropenone isotopomers with one ^{13}C may be more promising in the envelope of Sagittarius B2(N) because the ^{12}C to ^{13}C ratio in the Galactic center is as low as 20 to 30 (Müller et al. 2008, 2016; Halfen et al. 2017; Jacob et al. 2020).

We determined structural parameters of cyclopropenone which compare very favorably with those of cyclopropenylidene as far as comparison is possible. The CO bond length agrees almost exactly with that of formaldehyde. Relatively large deviations between our structural parameters and the earlier substitution structure were traced to misassignments of two transitions to the $^{13}\text{C}_2$ isotopolog which led to a too large A rotational parameter.

Acknowledgements. We are grateful to José Cernicharo for communication of unpublished results of a search for $c\text{-HDC}_3\text{O}$ in TMC-1. We acknowledge support by the Deutsche Forschungsgemeinschaft via the collaborative research center SFB 956 (project ID 184018867) project B3 as well as the Gerätezentrum SCHL 341/15-1 (“Cologne Center for Terahertz Spectroscopy”). We thank the Regionales Rechenzentrum der Universität zu Köln (RRZK) for provid-

ing computing time on the DFG funded High Performance Computing System CHEOPS. J.-C. G. is grateful for financial support by the Centre National d’Etudes Spatiales (CNES; grant number 4500065585) and by the Programme National Physique et Chimie du Milieu Interstellaire (PCMI) of CNRS/INSU with INC/INP co-funded by CEA and CNES. Our research benefited from NASA’s Astrophysics Data System (ADS).

References

- Anonymous. 1983, Chem. Eng. News, 61, 33
 Araki, M., Takano, S., Sakai, N., et al. 2017, ApJ, 847, 51
 Becke, A. D. 1993, J. Chem. Phys., 98, 5648
 Bell, M. B., Feldman, P. A., Matthews, H. E., & Avery, L. W. 1986, ApJ, 311, L89
 Benson, R. C., Flygare, W. H., Oda, M., & Breslow, R. 1973, J. Am. Chem. Soc., 95, 2772
 Berglund, M. & Wieser, M. E. 2011, Pure Appl. Chem., 83, 397
 Breslow, R. & Oda, M. 1972, J. Am. Chem. Soc., 94, 4787
 Breslow, R., Pecoraro, J., & Sugimoto, T. 1977, Org. Synth., 57, 41
 Cazzoli, G., Puzzarini, C., & Gauss, J. 2014, A&A, 566, A52
 Cernicharo, J., Marcelino, N., Agúndez, M., et al. 2020, A&A, 642, L17
 Costain, C. C. 1958, J. Chem. Phys., 29, 864
 Dunning, Jr., T. H. 1989, J. Chem. Phys., 90, 1007
 Epple, K. J. & Rudolph, H. D. 1992, J. Mol. Spectrosc., 152, 355
 Frisch, M. J., Trucks, G. W., Schlegel, H. B., et al. 2013, Gaussian 09, Revision E.01, Gaussian, Inc., Wallingford CT
 Gauss, J. & Stanton, J. F. 2000, J. Phys. Chem. A, 104, 2865
 Guillemin, J. C., Włodarczak, G., Lopez, J. C., & Demaison, J. 1990, J. Mol. Spectrosc., 140, 190
 Halfen, D. T., Woolf, N. J., & Ziurys, L. M. 2017, ApJ, 845, 158
 Harmony, M. D. 1990, J. Chem. Phys., 93, 7522
 Harmony, M. D. & Taylor, W. H. 1986, J. Mol. Spectrosc., 118, 163
 Hollis, J. M., Remijan, A. J., Jewell, P. R., & Lovas, F. J. 2006, ApJ, 642, 933
 Jacob, A. M., Menten, K. M., Wiesemeyer, H., et al. 2020, A&A, 640, A125
 Kania, P., Hermans, M., Brünken, S., Müller, H. S. P., & Giesen, T. F. 2011, J. Mol. Spectrosc., 268, 173
 Kraitchman, J. 1953, Am. J. Phys., 21, 17
 Lee, C., Yang, W., & Parr, R. G. 1988, Phys. Rev. B, 37, 785
 Liévin, J., Demaison, J., Herman, M., Fayt, A., & Puzzarini, C. 2011, J. Chem. Phys., 134, 064119
 Lohilahti, J. 2006, PhD thesis, University of Oulu, Oulu, Finland
 Loison, J.-C., Agúndez, M., Marcelino, N., et al. 2016, MNRAS, 456, 4101
 Lykke, J. M., Coutens, A., Jørgensen, J. K., et al. 2017, A&A, 597, A53
 Manigand, S., Coutens, A., Loison, J. C., et al. 2021, A&A, 645, A53
 Margulès, L., Motiyenko, R. A., & Demaison, J. 2020, J. Quant. Spectr. Rad. Transf., 253, 107153
 Martin, J. M. L. & Taylor, P. R. 1996, Chem. Phys. Lett., 248, 336
 Martin-Drumel, M. A., van Wijngaarden, J., Zingsheim, O., et al. 2015, J. Mol. Spectrosc., 307, 33
 Mills, I. M. 1972, in Molecular Spectroscopy: Modern Research, Volume 1, ed. K. N. Rao & C. W. Mathews, 115
 Møller, C. & Plesset, M. S. 1934, Phys. Rev., 46, 618
 Morgan, W. J., Matthews, D. A., Ringholm, M., et al. 2018, J. Chem. Theory Comput., 14, 1333

- Müller, H. S. P., Belloche, A., Menten, K. M., Comito, C., & Schilke, P. 2008, *J. Mol. Spectrosc.*, 251, 319
- Müller, H. S. P., Belloche, A., Xu, L.-H., et al. 2016, *A&A*, 587, A92
- Müller, H. S. P. & Gerry, M. C. L. 1994, *J. Chem. Soc., Faraday Trans.*, 90, 2601
- Müller, H. S. P., Maeda, A., Thorwirth, S., et al. 2019, *A&A*, 621, A143
- Müller, H. S. P., Zingsheim, O., Wehres, N., et al. 2017, *J. Phys. Chem. A*, 121, 7121
- Ordu, M. H., Müller, H. S. P., Walters, A., et al. 2012, *A&A*, 541, A121
- Peterson, K. A. & Dunning, Jr., T. H. 2002, *J. Chem. Phys.*, 117, 10548
- Pickett, H. M. 1991, *J. Mol. Spectrosc.*, 148, 371
- Raghavachari, K., Trucks, G. W., Pople, J. A., & Head-Gordon, M. 1989, *Chem. Phys. Lett.*, 157, 479
- Rudolph, H. D. 1991, *Struct. Chem.*, 2, 581
- Rudolph, H. D. 1995, in *Advances in Molecular Structure Research*, ed. I. Hargittai & M. Hargittai, Vol. 1 (JAI Press Inc., Greenwich, CT, USA), 63–114
- Spahn, H., Müller, H. S. P., Giesen, T. F., et al. 2008, *Chem. Phys.*, 346, 132
- Spezzano, S., Gupta, H., Brünken, S., et al. 2016, *A&A*, 586, A110
- Spezzano, S., Tamassia, F., Thorwirth, S., et al. 2012, *ApJS*, 200, 1
- Stanton, J. F., Lopreore, C. L., & Gauss, J. 1998, *J. Chem. Phys.*, 108, 7190
- Tamassia, F., Cané, E., Fusina, L., & Di Lonardo, G. 2016, *Phys. Chem. Chem. Phys.*, 18, 1937
- Wang, H.-J., von Ragué Schleyer, P., Wu, J. I., & Wang, H.-J. 2011, *Int. J. Quant. Chem.*, 111, 1031
- Watson, J. K. G. 1977, in *Vibrational spectra and structure*, 6, ed. J. R. Durig (Elsevier; Amsterdam), 1–89